Journal of Macromolecular Science, Part A
Publication details, including instructions for authors and subscription information:
http://www.informaworld.com/smpp/title~content=t713597274

Preparation and Characterization of Intercalated Polymethacrylamide/Na-Montmorillonite Nanocomposites

Meltem Çelı˙k[a]; Müşerref Önal[a]
[a] Department of Chemistry, Faculty of Science, Ankara University, Tandoğan, Ankara, Turkey

To cite this Article Çelı˙k, Meltem and Önal, Müşerref(2006) 'Preparation and Characterization of Intercalated Polymethacrylamide/Na-Montmorillonite Nanocomposites', Journal of Macromolecular Science, Part A, 43: 6, 933 — 943
To link to this Article: DOI: 10.1080/10601320600653806
URL: http://dx.doi.org/10.1080/10601320600653806

Journal of Macromolecular Science®, Part A: Pure and Applied Chemistry, 43:933–943, 2006

ISSN 1060-1325 print/1520-5738 online
DOI: 10.1080/10601320600653806

Preparation and Characterization of Intercalated Polymethacrylamide/Na-Montmorillonite Nanocomposites

MELTEM ÇELİK AND MÜŞERREF ÖNAL

Department of Chemistry, Faculty of Science, Ankara University, Tandoğan, Ankara, Turkey

Polymethacrylamide/Na-montmorillonite nanocomposites have been prepared by free-radical polymerization. All the nanocomposites were characterized by Fourier transform infrared spectroscopy, X-ray diffraction, scanning electron microscopy, thermogravimetric analysis, and differential thermal analysis. The thermal properties of nanocomposites are notably improved by the presence of the montmorillonite layers in comparison with pure polymethacrylamide. X-ray diffraction and scanning electron microscopy confirmed that polymethacrylamide could be easily inserted between the layers of Na-montmorillonite to form intercalated nanocomposites, and significantly large d-spacing expansions from 1.19 to 2.93 nm of the nanocomposites. Adsorptive properties of nanocomposites were also investigated.

Keywords nanocomposites, clay, polymethacrylamide, montmorillonite, free radical polymerization

Introduction

In recent years, polymer/clay nanocomposites have received a great deal of interest in many fields. These nanocomposites, as advanced structural materials, have excellent physical, mechanical and thermal properties compared with the pure polymer (1–4). Polymer/clay nanocomposites are a relatively new class of materials, with the particle size of the dispersed phase having less than 100 nm. Blends of thermoplastic polymers with montmorillonite have been extensively studied because a small amount of well dispersed clay in a polymer matrix can significantly improve its mechanical and thermal properties. Much research has been done in this field, and many polymer/clay nanocomposites have been synthesized with improved properties, including poly(vinyl chloride), polyurethane, polyamide 6, polypropylene, polystyrene, poly(methyl methacrylate), polyaniline, polybenzimidazole, poly(pyrrole) and poly(thiophene) (5–13).

Montmorillonite (MMT) has been widely used as a reinforcement filler for this purpose. The hydrophilic nature, small particle size, and layer expanding properties of the montmorillonite provide homogeneous dispersion in polymer matrix. The dispersion of clay into polymer matrix at nanometer-scale leads to significant improvements in the

Received November 2005; Accepted February 2006.
Address correspondence to Meltem Çelik, Department of Chemistry, Faculty of Science, Ankara University, 06100 Tandoğan, Ankara, Turkey. E-mail: mecelik@science.ankara.edu.tr

thermal, mechanical, and adsorptive properties of composites. The improved composites are widely used in areas such as transportation, construction materials, electronics and sporting goods and consumer products (14). Using clay for nanocomposites as inorganic fillers also reduces the cost.

Methacrylamide (MAA) is one of the most important vinyl monomers for large polymer-add-on can be easily obtained because of the hydrophilic nature of the MAA (15, 16). Polymethacrylamide (PMAA), as an important industrial polymer, has some desirable properties, including, it is less toxic, polar and less expensive than other vinyl monomers. Polymers based on methacrylamide with very high molecular weights have gained more and more technical attention due to the solubility in water. However, its biggest disadvantage is poor thermal and mechanical properties. Therefore, PMAA/Na-MMT nanocomposites offer the especially thermal stability.

In our previous works, we have synthesized the poly(glycidyl methacrylate)/Na-montmorillonite nanocomposites exhibiting good thermal stability and physical properties (17).

Therefore, the aim of this study is to exhibit the preparation and characterization of intercalated polymethacrylamide/Na-montmorillonite nanocomposites. The nanocomposites prepared were characterized by Fourier Transform Infrared Spectroscopy (FTIR), X-ray diffraction (XRD), scanning electron microscopy (SEM), thermogravimetric analysis (TGA), and differential thermal analysis (DTA). We also investigated and discussed adsorptive properties of nanocomposites.

Experimental

Materials

The sodium-montmorillonite (Na-MMT) clay, with a cation exchange capacity of 1.08 mol $kg,^{-1}$ was obtained from Reşadiye (Tokat/Turkey). It was used after further purification. The chemicals used in this study, including methacrylamide, benzoyl peroxide were purchased from Merck Chemical Company. The free radical initiator, benzoyl peroxide (Bz_2O_2) was recrystallized twice from methanol and chloroform mixture. All other chemicals were of chemically pure grade.

Purification of Clay

The original bentonite was ground to pass through a screen with a clear opening of 0.074 mm. The ground sample was dried at 105°C for 4 h. Na-rich montmorillonite was obtained by the methods of dispersion and sedimentation from its aqueous suspension (18).

Preparation of PMAA/Na-MMT Nanocomposites

A certain amount of Na-MMT was dispersed in 30 mL distilled water and dispersion was stirred overnight at room temperature. Then, at a suitable concentration MAA, and Bz_2O_2 as radical initiator (dissolved in 1 mL acetone) were added upon the dispersion. The resultant mixture was polymerized in a water bath (GFL-1003, Germany) and adjusted to the polymerization temperature (85°C) for 2 h to obtain polymethacrylamide/Na-MMT nanocomposites. After polymerization, obtained nanocomposites were washed

throughly with distilled water. The nanocomposites were then dried overnight in a vacuum oven at 40°C and weighed. The other samples were prepared by the same procedure using different concentrations of MAA. Codes and compositions of samples and the polymerization conditions are listed in Table 1.

Characterization of PMAA/Na-MMT Nanocomposites

The following methods were used to characterize the prepared nanocomposites.

Cation Exchange Capacity

The cation exchange capacity (CEC) is defined as the equivalent amount of exchanged cations in one kilogram of smectites (or in other cases, clays or clay minerals), were determined according to the methylene blue procedure (19–21). The CEC of the Na-MMT used was so determined as 1.08 mol kg^{-1}.

FTIR Spectra

FTIR spectra were recorded on pressed KBr pellets using a MATTSON 1000 Model FTIR spectrophotometer.

X-Ray Diffraction

XRD study of the samples was performed on a Philips PW 1730 powder diffractometer, using CuK radiation whose wavelength was 0.15418 nm, and a Ni filter was used.

Scanning Electron Microscopy

The morphology of the pure Na-MMT and composites was examined by a LEO-435 Model scanning electron microscope, after gold coating.

Table 1
Codes and chemical compositions of samples and polymerization conditions

Sample code	Monomer content (wt%)	Na-MMT content (wt%)
Pure Na-MMT	—	100.00
PMAA/Na-MMT1	42.86	57.14
PMAA/Na-MMT2	60.00	40.00
PMAA/Na-MMT3	71.43	28.57
PMAA/Na-MMT4	77.78	22.22
Pure PMAA	100.00	—

Bz_2O_2 concentration = 3.0×10^{-3} mol/L, temperature = 85°C, time = 2 h.

Thermogravimetric Analysis

A Shimadzu simultaneous DTA-TG apparatus (DTG-60H Model) thermal analyzer was used under the nitrogen gas flow of 100 mL/min. The temperature range studied was from room temperature to 1000°C at 10°C/min heating rate and α-Al_2O_3 was used as an inert material.

Adsorptive Properties

The adsorption and desorption isotherms of nitrogen at liquid nitrogen temperature for samples were also determined by a volumetric adsorption instrument, made of Pyrex glass, which was connected to high vacuum (22).

Results and Discussion

Dispersibility of Na-MMT in the PMAA Matrix

XRD is a conventional method to determine the interlayer spacing of the original clay and the intercalated polymer/clay nanocomposites (23).

Figure 1(a–e) shows the XRD results for the pure Na-MMT, pure PMAA, and PMAA/Na-MMT nanocomposites with different monomer contents. The *d*-spacings of the pure Na-MMT and nanocomposites before and after polymerization process are calculated using the Bragg's equation, $d = \lambda/2\sin\theta$. The initial *d*-spacing value (d_{001}) of the untreated Na-MMT was determined to be 1.19 nm. After polymerization process with PMAA, the diffraction patterns of PMAA/Na-MMT nanocomposites were higher with the increase of the MAA monomer content.

Also, the peak position and interlayer spacing results are presented in Table 2. The characteristic diffraction peak is at $2\theta = 3.01^\circ$ ($d_{001} = 2.93$ nm) for PMAA/Na-MMT4 (77.78 wt% monomer loading). These results demonstrate increased intercalation with increasing amount of the monomer. Increasing in the basal interlayer spacing is due to the insertion of polymer chains within the clay galleries.

This indicates that PMAA molecules are could diffuse into the interlayer space of clay and expand the interlayer spacing. In other words, an intercalated PMAA/Na-MMT nanocomposite has been synthesized.

Morphology

The dispersibility of the Na-MMT layers is also confirmed by scanning electron microscopy (SEM). Figure 2(a–c) displays SEM images of pure Na-MMT, and PMAA/Na-MMT nanocomposites containing 42.86 wt% and 77.78 wt% MAA, respectively. Figure 2(a) shows the morphology of individual layers of the Na-MMT before the intercalation. The change of morphology after intercalation with polymethacrylamide as illustrated in Figure 2(b) and (c). Examination of the images of the nanocomposites can be seen that the clay layers are dispersed uniformly and homogeneously in the polymer matrix and the Na-MMT interlayer spaces much larger. It is particularly interesting to note that the strong attaching of polymer to the Na-MMT surface due to the crosslinking between the Na-MMT layers. A related morphology has been observed for poly(styrene-maleic anhydride)-montmorillonite nanocomposite (24).

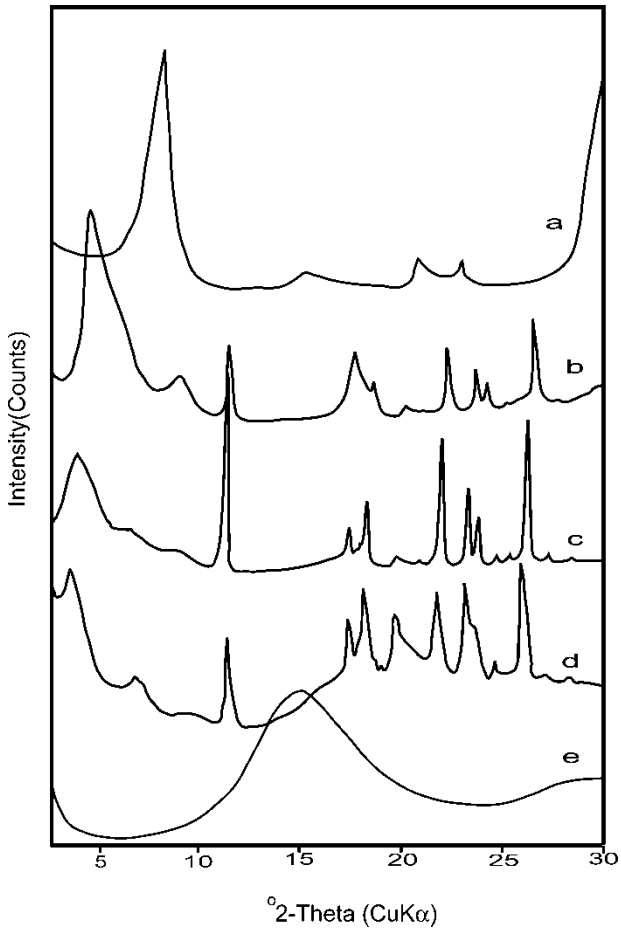

Figure 1. XRD patterns of pure Na-MMT, pure PMAA, and PMAA/Na-MMT nanocomposites: (a) pure Na-MMT, (b) PMAA/Na-MMT2 (60.00 wt% MAA), (c) PMAA/Na-MMT3 (71.43 wt% MAA), (d) PMAA/Na-MMT4 (77.78 wt% MAA), (e) pure PMAA.

Table 2
XRD data for pure Na-MMT, pure PMAA, and PMAA/Na-MMT nanocomposites

	Peak position	Interlayer spacing	Interlayer-expansion
Sample	2θ (°)	d_{001} (nm)	Δd_{001} (nm)
Pure Na-MMT	7.42	1.19	—
PMAA/Na-MMT2	4.22	2.09	0.90
PMAA/Na-MMT3	3.31	2.67	1.40
PMAA/Na-MMT4	3.01	2.93	1.74
Pure PMAA	15.06	0.59	—

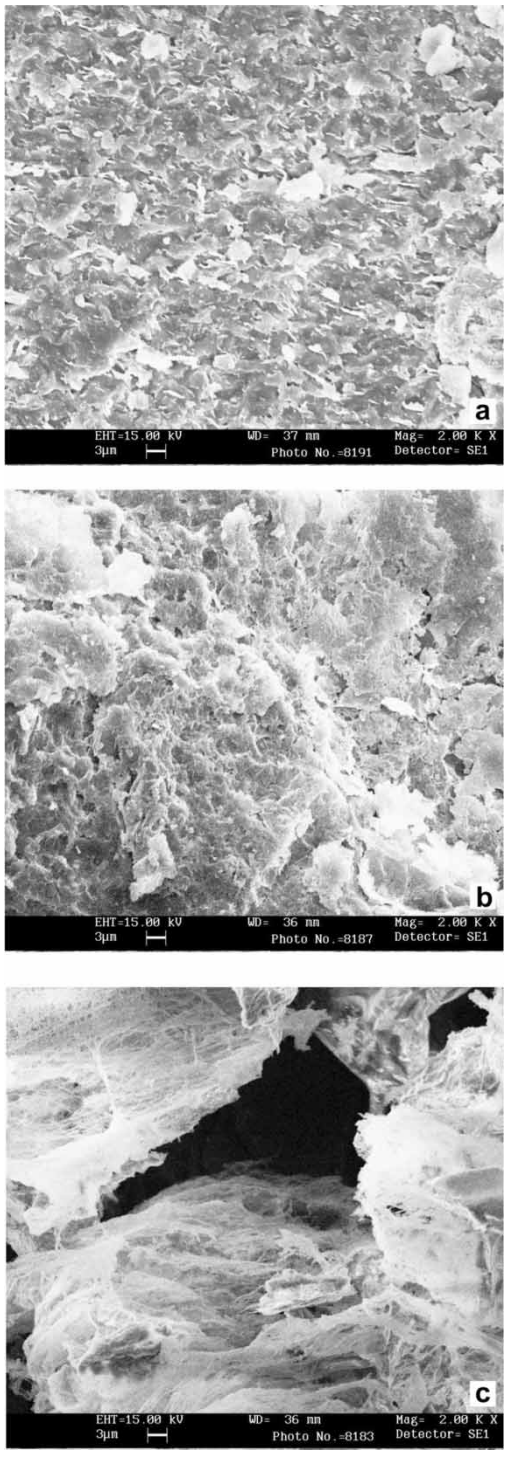

Figure 2. SEM micrographs of pure Na-MMT and PMAA/Na-MMT nanocomposites: (a) pure Na-MMT, (b) PMAA/Na-MMT1 (42.86 wt% MAA), (c) PMAA/Na-MMT4 (77.78 wt% MAA) at a magnification of $\times 2000$.

FTIR Analysis

FTIR spectra of pure Na-MMT, pure PMAA, and PMAA/Na-MMT4 nanocomposite (77.78 wt% MAA) are shown in Figure 3(a–c). Both pure PMAA and PMAA/Na-MMT4 nanocomposite have the characteristic bands of polymethacrylamide: 3193–3387 cm^{-1} (NH stretching), 1668 cm^{-1} (CO stretching), and 1605 cm^{-1} (CN stretching band). Besides these bands, PMAA/Na-MMT4 also has the characteristic bands of montmorillonite: 1030, 550, and 470 cm^{-1}, which corresponds to Si-O stretching vibrations, the stretching vibration of Al-O and bending of Si-O. This means PMAA has been intercalated into the layers of Na-MMT (15, 25).

Thermal Stability

Thermal stability is an important property for the nanocomposites. Pure Na-MMT, pure PMAA, and PMAA/Na-MMT2 (60.00 wt% MAA) were performed by TGA and DTA and results are shown in Figures 4 and 5. There are two major stages of the decomposition of pure Na-MMT (Figure 4(a)). The first weight loss below 130°C (≈5.63%) is a result of the evaporation of absorbed water. In the second stage of weight loss, water resulting from the structural –OH groups of Na-MMT begins to be removed. The total weight loss is only 15.82% up to 1000°C. As expected, the Na-MMT shows the highest thermal stability.

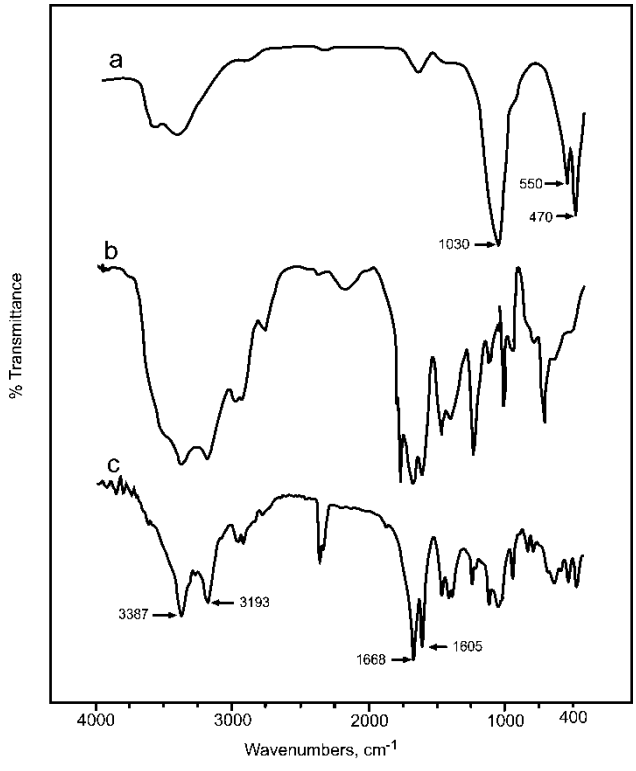

Figure 3. The FTIR spectra of pure Na-MMT, pure PMAA and PMAA/Na-MMT nanocomposite: (a) pure Na-MMT, (b) pure PMAA, (c) PMAA/Na-MMT4 (77.78 wt% MAA).

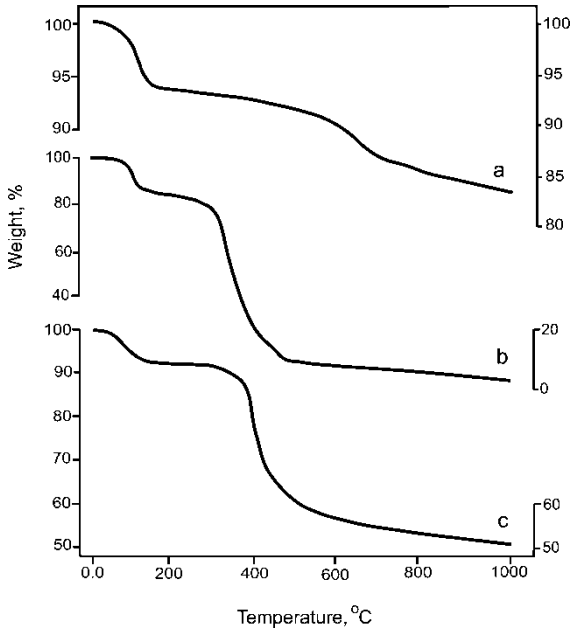

Figure 4. TGA curves of pure Na-MMT, pure PMAA, and PMAA/Na-MMT nanocomposite: (a) pure Na-MMT, (b) pure PMAA, (c) PMAA/Na-MMT2 (60.00 wt% MAA) obtained in nitrogen atmosphere at heating rate of 10°C/min.

Pure PMAA undergoes two degradation stages. For pure PMAA (Figure 4(b)), initial weight loss (≈15.46%) up to around 100°C is presumably due to the release of free water. The second stage is the thermal decomposition of polymer. As shown in Figure 4(b), the decomposition temperature of the pure PMAA is 350°C; its weight loss reaches

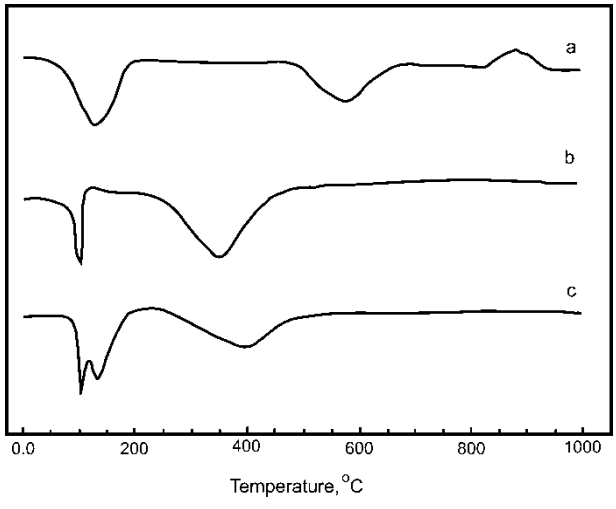

Figure 5. DTA curves of pure Na-MMT, pure PMAA and PMAA/Na-MMT nanocomposite: (a) pure Na-MMT, (b) pure PMAA, (c) PMAA/Na-MMT2 (60.00 wt% MAA) obtained in nitrogen atmosphere at heating rate of 10°C/min.

97.16% at 1000°C. Consequently, pure PMAA should exhibit lower thermal stability relative to pure Na-MMT.

The TGA curve of PMAA/Na-MMT2 nanocomposite confirms that the enhanced thermal stability of intercalated polymer (Figure 4(c)). As a comparison, the TGA curve of PMAA/Na-MMT2 nanocomposite shows a two-step weight loss. The first weight loss ranging from 50 to 200°C is attributed to the loss of water and the second weight loss is the thermal decomposition of the nanocomposite. The PMAA/Na-MMT2 nanocomposite has a higher decomposition temperature (400°C) than that of pure PMAA. In other words, the thermal decomposition temperature of nanocomposite is 50°C higher than that of pure PMAA. The weight loss of the PMAA/Na-MMT2 nanocomposite decreased to a value of 49.59% at 1000°C. It is notable that only a small amount of Na-MMT is effective in improving the residual wt% and lowering thermal degradation rate for nanocomposite. This enhancement in the thermal stability is due to the fact that the introduction of a well-dispersed Na-MMT can prevent the heat from transmitting quickly and then improve the thermal stability of the nanocomposite (6).

In the DTA curve of the pure Na-MMT, the endothermic peaks, which result from dehydration (around 130°C), dehydroxylation (500–700°C), and the exothermic peak (850–950°C) results from recrystallization are observed (Figure 5(a)). Pure PMAA shows the endothermic peaks, which corresponds to dehydration (100°C) and the structure starts to decompose at 350°C (Figure 5(b)). Figure 5(c) indicates that, in the nanocomposite, the twin peaks occurring nearly at 100°C and 130°C result from the dehydration of PMAA and Na-MMT, respectively. In Figure 5(c), the endothermic peak of 350°C at Figure 5(b) for pure PMAA shifted to 400°C, which indicates that the decomposition of PMAA at nanocomposite occurs at higher temperatures of 50°C. In Figure 5(c), the dehydroxylation endothermic and recrystallization exothermic peaks of Figure 5(a)

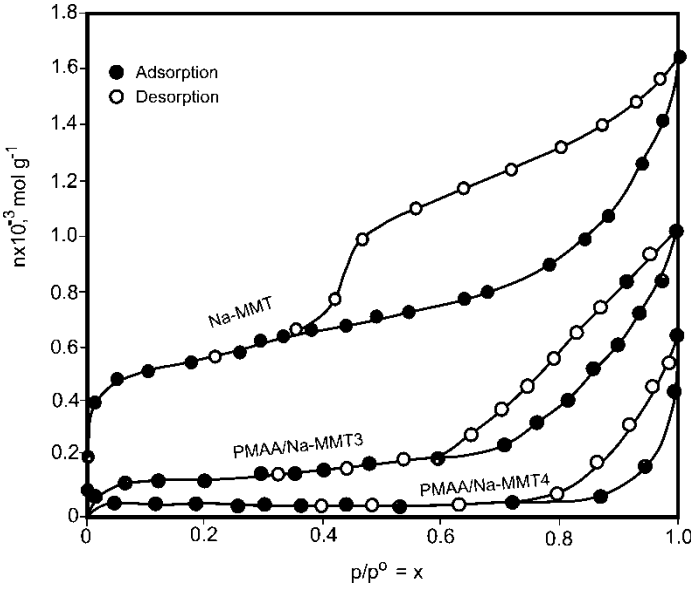

Figure 6. The adsorption and desorption isotherms of the nitrogen on the pure Na-MMT and PMAA/Na-MMT nanocomposites.

Table 3
The specific surface areas (S_{BET}) and specific micro-mesopore volumes of the pure Na-MMT and PMAA/Na-MMT nanocomposites

Sample	(S_{BET}), m^2g^{-1}	V, cm^3g^{-1}
Pure Na-MMT	42.0	0.07
PMAA/Na-MMT3	11.0	0.04
PMAA/Na-MMT4	3.0	0.02

at 500–700°C and 850–950°C, respectively could not be observed at nanocomposite. This fact indicates that the dehydroxylation and recrystallization properties of Na-MMT in polymer as nanoparticles have disappeared. The TGA curves at Figure 4(c) also support this fact.

Adsorptive Properties

The adsorption and desorption isotherms of the nitrogen on pure Na-MMT and PMAA/Na-MMT nanocomposites are given in Figure 6. Here, p is the adsorption equilibrium pressure, p° is the saturated vapour pressure of liquid nitrogen, $p/p^\circ \equiv x$ is the relative equilibrium pressure, and n ($molg^{-1}$), defined as molar amount of nitrogen adsorbed one gram of sample, is the adsorption capacity.

As could be expected, the pure Na-MMT shows the highest adsorption capacity. Figure 6 also shows that, adsorption capacity of PMAA/Na-MMT nanocomposites increases with the amount of clay in the nanocomposite.

The specific surface areas (S_{BET}) for pure Na-MMT and PMAA/Na-MMT nanocomposites were calculated according to the Brunauer-Emmett-Teller (BET) equation (26) by using the nitrogen adsorption data in Figure 6 and were listed in Table 3. The specific micro-mesopore volumes (V) were determined from the desorption data in Figure 6 and were listed in Table 3.

The BET specific surface area and specific micro-mesopore volume of the pure Na-MMT was $42.0\,m^2g^{-1}$ and $0.07\,cm^3g^{-1}$, respectively (Table 3). For higher loading of PMAA, the BET specific surface area and specific micro-mesopore volume were notably decreased to $3.0\,m^2g^{-1}$ and $0.02\,cm^3g^{-1}$, respectively. This could be described by the fact that the delamation following intercalation during the formation of nanocomposite leads a decrease in porosity and surface area. Also the polymer covered Na-MMT nanoparticles can not adsorb nitrogen molecules which indicates that the diffusion of nitrogen molecules is restricted by polymer (17).

Conclusions

We synthesized the nanocomposites of MAA and Na-MMT clay through the free-radical polymerization method. X-ray diffraction and scanning electron microscopy confirmed that polymethacrylamide (PMAA) could be easily inserted between the layers of Na-montmorillonite to form intercalated nanocomposites. The intercalation of polymethacrylamide into the galleries of the clay was confirmed by X-ray diffraction analysis, and, significantly large d-spacing expansions from 1.19 to 2.93 nm for the nanocomposites

were observed. Thermal properties of the samples were studied by thermogravimetric analysis and differential thermal analysis. From the TGA and DTA results, we observed that, in comparison with pure PMAA, the thermal properties nanocomposites are notably improved by the presence of the nanometric clay layers. The weight loss% of PMAA/Na-MMT nanocomposites was obviously less than that of the pure PMAA. In addition, the adsorptive properties of nanocomposites were obviously increased compared to that of pure PMAA, whereas these properties were decreased compared to that of pure Na-MMT.

Acknowledgements

The work was financially supported by the Ankara University Research Fund (Project Number 20040705040) and by the Turkish Scientific and Research Institute (Project Number 104T094).

References

1. Xia, X., Yih, J., D'Souza, N.A., and Hu, Z. (2003) *Polymer*, 44: 3389–3393.
2. Hasegawa, N., Okamoto, H., Kawasumi, M., and Usuki, A. (1999) *J. Appl. Polym. Sci.*, 74: 3359–3364.
3. Someya, Y., Nakazato, T., Teramoto, N., and Shibata, M. (2004) *J. Appl. Polym. Sci.*, 91: 1463–1475.
4. Zhu, J. and Wilkie, C.A. (2000) *Polym. Int.*, 49: 1158–1163.
5. Ren, J., Huang, Y., Liu, Y., and Tang, X. (2005) *Polymer Test.*, 24: 316–323.
6. Han, B., Cheng, A., Ji, G., Wu, S., and Shen, J. (2004) *J. Appl. Polym. Sci.*, 91: 2536–2542.
7. Liu, X., Wu, Q., Berglund, L.A., and Qi, Z. (2002) *Macromol. Mater. Eng.*, 287: 515–522.
8. Pehlivan, H., Özmıhçı, F., Tıhmınlıoğlu, F., Balköse, D., and Ülkü, S. (2003) *J. Appl. Polym. Sci.*, 90: 3069–3075.
9. Fu, X. and Qutubuddin, S. (2000) *Mater Lett.*, 42: 12–15.
10. Liu, G.D., Zhang, L.C., Qu, X.W., Wang, B.T., and Zhang, Y. (2003) *J. Appl. Polym. Sci.*, 90: 3690–3695.
11. Wu, Q., Xue, Z., Qi, Z., and Wang, F. (2000) *Polymer*, 41: 2029–2032.
12. Gültek, A., I.çduygu, M.G., and Seçkin, T. (2004) *Mater Sci. Eng. B.*, 107: 166–171.
13. Oriakhi, C.O. and Lerner, M.M. (1995) *Mater Res. Bull.*, 30: 723–729.
14. Fu, X. and Qutubuddin, S. (2001) *Polymer*, 42: 807–813.
15. Önal, M. and Çelik, M. (2006) *Mater Lett.*, 60: 48–52.
16. Çelik, M. (2004) *J. Appl. Polym. Sci.*, 94: 1519–1525.
17. Çelik, M. and Önal, M. (2004) *J. Appl. Polym. Sci.*, 94: 1532–1538.
18. Önal, M., Sarıkaya, Y., Alemdaroğlu, T., and Bozdoğan, I. (2003) *Turk J. Chem.*, 27: 683–694.
19. Rytwo, G., Serben, C., Nir, S., and Margulies, L. (1991) *Clays Clay Miner.*, 39: 551–555.
20. Hang, P.T. and Brindley, G.W. (1970) *Clays Clay Miner.*, 18: 203–312.
21. Sarıkaya, Y., Önal, M., Baran, B., and Alemdaroğlu, T. (2000) *Clays Clay Miner.*, 48: 557–562.
22. Önal, M., Sarıkaya, Y., and Alemdaroğlu, T. (2001) *Turk J. Chem.*, 25: 241–249.
23. Chang, J.H., An, Y.U., Cho, D., and Giannelis, E.P. (2003) *Polymer*, 44: 3715–3720.
24. Salahuddin, N. and Akelah, A. (2002) *Polym. Adv. Technol.*, 13: 339–345.
25. Zhang, X., Xu, R., Wu, Z., and Zhou, C. (2003) *Polym. Int.*, 52: 790–794.
26. Brunauer, S., Emmett, P.H., and Teller, E. (1938) *J. Am. Chem. Soc.*, 60: 308–319.